



UNIVERSITI PUTRA MALAYSIA

**SYNTHESIS AND CHARACTERISATION OF VANADIUM
PHOSPHOROUS OXIDE CATALYSTS**

LOOI MING HOONG.

FSAS 2004 19

**SYNTHESIS AND CHARACTERISATION OF VANADIUM
PHOSPHOROUS OXIDE CATALYSTS**

LOOI MING HOONG

**DOCTOR OF PHILOSOPHY
UNIVERSITI PUTRA MALAYSIA**

2004



**SYNTHESIS AND CHARACTERISATION OF VANADIUM PHOSPHOROUS
OXIDE CATALYSTS**

By

LOOI MING HOONG

**Thesis Submitted to the School of Graduate Studies, Universiti Putra Malaysia in
Fulfilment of the Requirement for the Degree of Doctor of Philosophy**

February 2004



Specially dedicated to

*Husband, McCool, Anderson, Chawla, Clark, Ramon and Brown
the seven brave souls who perished on board the Columbia.*



Abstract of thesis presented to the Senate of Universiti Putra Malaysia in fulfilment of the requirements for Doctor of Philosophy

**SYNTHESIS AND CHARACTERISATION OF VANADIUM PHOSPHOROUS
OXIDE CATALYSTS**

By

LOOI MING HOONG

February 2004

Chairman: Taufiq Yap Yun Hin, Ph.D.

Faculty: Science and Environmental Studies

The V/P/O catalysts were prepared by using (a) organic method (VPO); (b) via dihydrate phase (VPD) and (c) aqueous method (VPA). The effect of calcination time, preparation method and addition of metal cations as dopants to the physico-chemical properties were studied using nitrogen physisorption measurements, scanning electron microscopy (SEM), X-ray diffraction, inductively coupled plasma (ICP) spectroscopy, redox titration, temperature programmed desorption (TPD) and temperature programmed reduction (TPR).

Surface areas of these mesoporous vanadium phosphorous oxides were apparently influenced by the length of calcination time, preparation method and incorporation of metal cations. The changes of surface areas were related to the changes of surface and bulk morphologies as evidenced by SEM.

X-ray diffraction revealed that while all of the V/P/O were consisted of predominantly V^{4+} phase of $(VO)_2P_2O_7$, minority V^{5+} phase which resumed many crystalline forms made up the remaining portion. Addition of metal cations to the basic matrix resulted



in slight loss of crystallinity for V/P/O by VPO method but a huge effect to V/P/O by VPD method which also accompanied by a marked increase in lattice strains.

Average oxidation state of vanadium (determined by redox titration) can be altered by (i) increase time of calcinations, (ii) predisposed by the preparation method and (iii) incorporation of metal cations.

The persistently lowering of the amount of oxygen atoms that were available thermally until stabilisation at around half a monolayer suggests that the catalytic activity, and hence the conversion of hydrocarbon is stabilised after 100 h. From the extra peak that appeared at higher temperature during TPR by H₂ for V/P/O calcined for longer duration, it was postulated that the selective nature of equilibrated V/P/O is originated from these oxygen atoms.

Based on the above argument, it was suggested that the VPD type of preparation would result in V/P/O with more active and selective nature than VPO and VPA. The addition of metal cations to bulk VPO was shown to increase the activity in the order of Zn > VPO (bulk) > Cr > Co and selectivity in the order of Co > Cr > Zn > VPO (bulk). While for VPD the activity and selectivity will be in the order of Co > VPD (bulk) > Cr > Zn and Zn > Cr > VPD (bulk) \approx Co, respectively.

Abstrak thesis yang dikemukakan kepada Senat Universiti Putra Malaysia sebagai memenuhi keperluan untuk Doktor Falsafah

SINTESIS DAN PENCIRIAN MANGKIN VANADIUM FOSFORUS OKSIDA

Oleh

LOOI MING HOONG

Februari 2004

Pengerusi: Taufiq Yap Yun Hin, Ph.D.

Fakulti: Sains dan Pengajian Alam Sekitar

Mangkkin V/P/O telah disintesis dengan menggunakan (a) kaedah organik (VPO); (b) melalui fasa dihidrat (VPD) dan (c) kaedah akuas (VPA). Kesan daripada tempoh pengkalsinan, kaedah sintesis dan penambahan kation-kation logam sebagai penggalak kepada ciri-ciri fiziko-kimia telah dikaji dengan menggunakan kaedah fizijerapan nitrogen, mikroskop imbasan elektron (SEM), pembelauan sinar-X, spektroskopi plasma pasangan induktif (ICP), penitratan redoks, penyahjerapan suhu berprogram (TPD) dan penurunan suhu berprogram (TPR).

Luas permukaan oksida-oksida vanadium fosforus yang berciri liang meso ini dipengaruhi oleh tempoh pengkalsinan, cara sintesis dan juga penambahan kation-kation logam. Perubahan luas permukaan ini boleh dikaitkan dengan perubahan morfologi permukaan dan pukal seperti yang dikesan oleh SEM.

Pembelauan sinar-X menunjukkan bahawa semua V/P/O terdiri daripada fasa V^{4+} dalam bentuk $(VO)_2P_2O_7$ sebagai fasa majority dan fasa minoriti V^{5+} yang mempunyai pelbagai bentuk kristal. Sel unit untuk prekursor dan mangkkin telah ditentukan sebagai ortorombik dengan pemalar-pemalar kekisi yang menyerupai bahan piawai.

Penambahan kation-kation logam kepada matriks asas menyebabkan sedikit pengurangan dalam kekristalan untuk V/P/O yang disintesis melalui kaedah VPO. Kesan yang nyata kepada sifat kekristalan dan penambahan regangan kekisi V/P/O dengan kaedah VPD telah diperhatikan.

Keadaan pengoksidaan purata untuk vanadium (dengan penitratan redoks) boleh diubah dengan (i) menambahkan tempoh pengkalsinan, (ii) kaedah sintesis dan (iii) penambahan kation-kation logam.

Atom-atom oksigen yang diperolehi secara terma sentiasa berkurangan sehingga tahap stabil pada lebih kurang setengah mono-lapisan mencadangkan bahawa aktiviti mangkin dan seterusnya penukaran hidrokarbon akan stabil selepas 100 j. Daripada puncak tambahan yang muncul pada suhu yang lebih tinggi semasa TPR dengan hydrogen untuk V/P/O yang dikalsinkan dalam masa yang lebih panjang, cadangan bahawa sifat pemilihan V/P/O dalam keadaan keseimbangan berasal daripada atom-atom oksigen ini telah dibuat.

Berasaskan kepada perbincangan di atas, kaedah VPD akan menghasilkan V/P/O yang bersifat lebih aktif dan pemilih daripada kaedah VPO dan VPA. Penambahan kation-kation logam kepada pukal VPO akan meningkatkan aktiviti dalam susunan $Zn > VPO$ (pukal) $> Cr > Co$ dan pemilihan dalam susunan $Co > Cr > Zn > VPO$ (pukal). Semetara untuk VPD pula, aktiviti dan pemilihan akan berada dalam susunan $Co > VPD$ (pukal) $> Cr > Zn$ dan $Zn > Cr > VPD$ (pukal) $\approx Co$ masing-masing.

ACKNOWLEDGEMENTS

First of all, I would like to thank my loving parents for their unconditional love, care and support throughout the years. I also owe my thanks to my sisters and brother who always stand by me.

I would like to acknowledge gratefully my principle supervisor Associate Professor Dr. Taufiq Yap Yun Hin for his excellent guidance, invaluable suggestions and help rendered throughout this research work. I would also like to thank my co-supervisors Professor Dr. Mohd. Zobir bin Hussein and Associate Professor Dr. Zulkarnain bin Zainal for their patience, help and advice all along.

My high appreciation to the cooperation from all the administrative staff and all the technicians in the laboratories in the Department of Chemistry and the Faculty of Science and Environmental Studies who are always there to help. The School of Graduate Studies which has provided assistance for the postgraduate program is also acknowledged.

The financial support by the Ministry of Science, Technology and Environment, Malaysia under IRPA grant is acknowledged. Scholarship in the form of PASCA Postgraduate Fellowship Scheme is also gratefully acknowledged.

My gratitude is also extended to Dr. Luca Lucarelli of Thermo Finnigan, Milan, Italy for his assistance in running the temperature-programmed desorption (TPD) of oxygen and reduction (TPR) by hydrogen analysis. I would also like to thank Mr



Guee Eng Hwa and Madam Rafizah binti Budin of O'Connor's Engineering Sdn. Bhd. for facilitating the correspondence with Dr. Lucarelli. My acknowledgement is also due to Mr. Zaimi bin Naim and Ms. Shamsina binti Sabdin of Petronas Research & Scientific Services Sdn. Bhd. for completing part of the TPD and TPR analysis.

Last but not least, I would like to thank all my friends, particularly Vee Min, Kia Chet and Pooi Wooi, and colleagues of Catalysis Laboratory (Lab 1) and Material Science Laboratory (Lab 2) for their help, advice and moral support.



I certify that an Examination Committee met on 12th February 2004 to conduct the final examination of Looi Ming Hooi on his Doctor of Philosophy thesis entitled "Synthesis and Characterisation of Vanadium Phosphorous Oxide Catalysts" in accordance with Universiti Pertanian Malaysia (Higher Degree) Act 1980 and Universiti Pertanian Malaysia (Higher Degree) Regulations 1981. The Committee recommends that the candidate be awarded the relevant degree. Members of the Examination Committee are as follows:

Irmawati binti Ramli, Ph.D.

Lecturer
Faculty of Science and Environmental Studies
Universiti Putra Malaysia
(Chairman)

Taufiq Yap Yun Hin, Ph.D.

Associate Professor
Faculty of Science and Environmental Studies
Universiti Putra Malaysia
(Member)

Mohd. Zobir bin Hussein, Ph.D.

Professor
Faculty of Science and Environmental Studies
Universiti Putra Malaysia
(Member)

Zulkarnain bin Zainal, Ph.D.

Associate Professor
Faculty of Science and Environmental Studies
Universiti Putra Malaysia
(Member)

Ambar bin Yarmo, Ph.D.

Associate Professor
Faculty of Science
Universiti Kebangsaan Malaysia
(Independent Examiner)



GULAM RUSUL RAHMAT ALI, Ph.D.

Professor/Deputy Dean
School of Graduate Studies
Universiti Putra Malaysia

Date: **27 MAY 2004**



This thesis submitted to the Senate of Universiti Putra Malaysia and has been accepted as fulfillment of the requirements for the degree of Doctor of Philosophy. The members of the Supervisory Committee are as follows:

Taufiq Yap Yun Hin, Ph.D.


Associate Professor,
Faculty of Science and Environmental Studies,
Universiti Putra Malaysia
(Chairman)

Mohd. Zobir bin Hussein, Ph.D,

Professor,
Faculty of Science and Environmental Studies,
Universiti Putra Malaysia.
(Member)

Zulkarnain bin Zainal, Ph.D,

Associate Professor,
Faculty of Science and Environmental Studies,
Universiti Putra Malaysia.
(Member)



AINI IDERIS, Ph.D,
Professor/ Dean,
School of Graduate Studies,
Universiti Putra Malaysia.

Date: 16 JUN 2004

DECLARATION FORM

I hereby declare that the thesis is based on my original work except for quotations and citations which have been duly acknowledged. I also declare that it has not been previously or concurrently submitted for any other degree at UPM or other institutions.



LOO MING HOONG

Date: 7 JUNE 2004

TABLE OF CONTENTS

	Page
ABSTRACT	iii
ABSTRAK	v
ACKNOMLEDGEMENTS	vii
APPROVAL	ix
DECLARATION	xi
LIST OF TABLES	xv
LIST OF FIGURES	xx
LIST OF ABBREVIATIONS	xxv

CHAPTER

1	INTRODUCTION	
1.1	Catalyst and Catalysis	1
1.2	Classification of Catalyst	2
1.3	General Requirements for Industrial Catalysts	3
1.4	Selective Oxidation Reactions	4
1.4.1	Dehydrogenation Reactions	4
1.4.2	Oxygenate Insertion	6
1.4.3	Dehydrogenation and Oxygen Insertion	7
1.4.4	Principle Properties for Selective Oxidation Catalysts	8
1.5	Maleic Anhydride	10
1.6	Objectives and Scope of this Thesis	13
2	LITERATURE REVIEW	
2.1	Feedstock	15
2.2	<i>n</i> -Butane Route-Background and Historical Development	16
2.3	Vanadyl Phosphorous Oxide (V/P/O) Catalyst	19
2.3.1	Preparation method of V/P/O	23
2.3.2	Influence of P:V Ratio	27
2.3.3	Influence of Activation Procedure	31
2.3.4	The effect of Dopant Addition	36
2.4	Presence of Defects as Active Site	47
3	EXPERIMENTAL	
3.1	Material and Gases	49
3.2	Preparation of Bulk (VO) ₂ P ₂ O ₇ Catalysts	50
3.2.1	Organic Route (VPO)	50
3.2.2	Reduction of VOPO ₄ ·2H ₂ O Phase (VPD)	51
3.2.3	Aqueous Route (VPA)	52



3.3	Preparation of Promoted Catalysts	53
3.3.1	Organic Route	53
3.3.2	Reduction of VOPO ₄ ·2H ₂ O Phase	54
3.4	Catalysts Characterizations	55
3.4.1	Nitrogen physisorption measurements	55
3.4.2	Scanning Electron Microscopy (SEM)	58
3.4.3	X-ray Diffraction (XRD)	59
3.4.4	Inductively Coupled Plasma-Emission Spectroscopy (ICP-AES)	61
3.4.5	Redox Titration	63
3.4.6	Temperature Programmed Desorption of Oxygen	66
3.4.7	Temperature Programmed Reduction by Hydrogen	67
3.4.8	Temperature Programmed Reaction with <i>n</i> -Butane	68
4	EFFECT OF THE ACTIVATION DURATION ON THE MORPHOLOGY AND REACTIVITY OF V/P/O CATALYSTS	
4.1	Introduction	70
4.2	BET Surface Area Measurements and Chemical Compositions	71
4.3	Surface Morphology	72
4.4	Crystallography Studies	74
4.4.1	Phase Identification	74
4.4.2	Lattice Constants and Stress-Strain Analysis	78
4.5	Oxygen Behaviour	83
4.5.1	Temperature-Programmed Desorption	83
4.5.2	Temperature-Programmed Reduction	87
4.6	Conclusions	92
5	EFFECT PREPARATION METHOD TO THE PHYSICO-CHEMICAL PROPERTIES OF V/P/O CATALYSTS	
5.1	Introduction	94
5.2	BET Surface Area Measurements and Chemical Compositions	95
5.3	Surface Morphology	96
5.4	Crystallography Studies	98
5.4.1	Phase Identification	98
5.4.2	Lattice Constants and Stress-Strain Analysis	103
5.5	Oxygen Behaviour	106
5.5.1	Temperature-Programmed Desorption	106
5.5.2	Temperature-Programmed Reduction	110
5.6	Conclusions	114

6	EFFECT OF PROMOTERS TO THE PHYSICO-CHEMICAL PROPERTIES OF PRECURSORS AND CATALYSTS	
6.1	Introduction	117
6.2	BET Surface Area Measurements and Chemical Compositions	118
6.3	Surface Morphology	121
6.4	Crystallography Studies	123
6.4.1	Phase Identification	123
6.4.2	Lattice Constants and Stress-Strain Analysis	132
6.5	Oxygen Behaviour	138
6.5.1	Temperature-Programmed Desorption	138
6.5.2	Temperature-Programmed Reduction	144
6.5.3	Temperature-Programmed Reaction	150
6.6	Conclusions	156
	REFERENCES	159
	APPENDIX	170
	BIODATA OF THE AUTHOR	238



LIST OF TABLES

Table		Page
1.1	Oxidation Catalysis in Industry.	5
1.2	Some Common Oxide Catalysed Selective Oxidation Reactions.	10
1.3	World maleic anhydride capacity (in metric tonnes) by reactor type.	11
1.4	Total world production of maleic anhydride (1000 metric tonnes).	12
1.5	Maleic anhydride consumption in the United States for the year 2000.	13
4.1	BET surface areas and chemical analysis of V/P/O catalysts at different calcinations duration.	71
4.2	Relative intensities and intensity ratios of (200) and (042) reflection plane of the pseudo-equilibrated catalysts.	77
4.3	Comparison of lattice parameters of VPOP with a standard.	79
4.4	Comparison of lattice parameters of standard with VPO40, VPO100 and VPO132.	79
4.5	Average crystallite size, microstrain and crystallite sizes at the (001) and (220) diffractions for the VPOP.	82
4.6	Average crystallite sizes and microstrains and crystallite sizes at (200) and (024) directions for the catalysts.	83
4.7	Total number of oxygen atoms desorbed from the catalysts by O ₂ TPD and the derived desorption activation energy	85
4.8	Total number of oxygen atoms removed from the catalysts by H ₂ and the derived reduction activation energy	89
5.1	BET surface areas and chemical analysis of V/P/O catalysts prepared by different preparation method.	95
5.2	Relative intensities and intensity ratios of (200) and (042) reflection plane of the pseudo-equilibrated catalysts.	103
5.3	Comparison of lattice parameters of precursors with a standard.	103
5.4	Comparison of lattice parameters of standard with VPD75, VPO75 and VPA75.	104



5.5	Average crystallite size, microstrain and crystallite sizes at the (001) and (220) diffractions for the precursors.	105
5.6	Average crystallite sizes and microstrains and crystallite sizes at (200) and (024) directions for the catalysts.	106
5.7	Total number of oxygen atoms desorbed from the catalysts by O ₂ TPD and the derived desorption activation energy.	108
5.8	Total number of oxygen atoms removed from the catalysts by H ₂ TPR and the derived reduction activation energy.	112
6.1	BET surface areas and chemical analysis of doped VPO and VPD catalysts.	118
6.2	Relative intensities and intensity ratios of (200) and (024) reflection plane of the doped VPO catalysts.	129
6.3	Relative intensities and intensity ratios of (200) and (024) reflection plane of the doped VPO catalysts.	132
6.4	Comparison of lattice parameters of undoped and the doped VPO precursors.	133
6.5	Comparison of lattice parameters of undoped and the doped VPD precursors.	134
6.6	Average crystallite sizes, microstrains and crystallite sizes at the (001) and (220) diffractions for the doped precursors.	136
6.7	Average crystallite sizes, microstrains and crystallite sizes at the (200) and (024) diffractions for the doped catalysts.	137
6.8	Total number of oxygen atoms desorbed from the doped VPO catalysts by O ₂ TPD and the derived desorption activation energy.	140
6.9	Total number of oxygen atoms desorbed from the doped VPD catalysts by O ₂ TPD and the derived desorption activation energy.	143
6.10	Total number of oxygen atoms removed from the doped VPO catalysts by H ₂ and the derived reduction activation energy.	147
6.11	Total number of oxygen atoms removed from the doped VPD catalysts by H ₂ and the derived reduction activation energy.	149
6.12	The m/z ratios followed to identify the compound cited.	154
6.13	Selectivity of products from TPR _n of <i>n</i> -butane over VPOCo ₂ ,	155



VPOCr2 and VPDCr2.

A.1	Determination of lattice parameter of VPOP using Lipson's method.	172
A.2	Determination of lattice parameter of VPO40 using Lipson's method.	172
A.3	Determination of lattice parameter of VPO100 using Lipson's method.	173
A.4	Determination of lattice parameter of VPO132 using Lipson's method.	173
A.5	Determination of lattice parameter of VPDP using Lipson's method.	174
A.6	Determination of lattice parameter of VPOP using Lipson's method.	174
A.7	Determination of lattice parameter of VPAP using Lipson's method.	175
A.8	Determination of lattice parameter of VPD75 using Lipson's method.	175
A.9	Determination of lattice parameter of VPO75 using Lipson's method.	176
A.10	Determination of lattice parameter of VPA75 using Lipson's method.	176
A.11	Determination of lattice parameter of VPOCo2P using Lipson's method.	177
A.12	Determination of lattice parameter of VPOCr2P using Lipson's method.	177
A.13	Determination of lattice parameter of VPOZn2P using Lipson's method.	178
A.14	Determination of lattice parameter of VPDCo2P using Lipson's method.	178
A.15	Determination of lattice parameter of VPDCr2P using Lipson's method.	179
A.16	Determination of lattice parameter of VPDZn2P using Lipson's method.	179



A.17	Determination of lattice parameter of VPOCo ₂ using Lipson's method.	180
A.18	Determination of lattice parameter of VPOCr ₂ using Lipson's method.	180
A.19	Determination of lattice parameter of VPOZn ₂ using Lipson's method.	180
A.20	Determination of lattice parameter of VPDCo ₂ using Lipson's method.	181
A.21	Determination of lattice parameter of VPDCr ₂ using Lipson's method.	181
A.22	Determination of lattice parameter of VPDZn ₂ using Lipson's method.	181
C.1	Data treatment for calculation of desorption activation energy, E_d of VPO40.	207
C.2	Data treatment for calculation of desorption activation energy, E_d of VPO100.	208
C.3	Data treatment for calculation of desorption activation energy, E_d of VPO132.	209
C.4	Data treatment for the calculation of desorption activation energy, E_d of VPD75.	210
C.5	Data treatment for the calculation of desorption activation energy, E_d of VPO75.	211
C.6	Data treatment for the calculation of desorption activation energy, E_d of VPA75.	212
C.7	Data treatment for the calculation of desorption activation energy, E_d of VPOCo ₂ .	213
C.8	Data treatment for the calculation of desorption activation energy, E_d of VPOCr ₂ .	214
C.9	Data treatment for the calculation of desorption activation energy, E_d of VPOZn ₂ .	215
C.10	Data treatment for the calculation of desorption activation energy, E_d of VPDCo ₂ .	216
C.11	Data treatment for the calculation of desorption activation	217



	energy, E_d of VPDCr2.	
C.12	Data treatment for the calculation of desorption activation energy, E_d of VPDZn2.	218
D.1	Data treatment for calculation of reduction activation energy, E_r of VPO40.	219
D.2	Data treatment for calculation of reduction activation energy, E_r of VPO100.	220
D.3	Data treatment for calculation of reduction activation energy, E_r of VPO132.	221
D.4	Data treatment for the calculation of reduction activation energy, E_r of VPD75.	222
D.5	Data treatment for the calculation of reduction activation energy, E_r of VPO75.	223
D.6	Data treatment for the calculation of reduction activation energy, E_r of VPA75.	224
D.7	Data treatment for the calculation of reduction activation energy, E_r of VPOCo2.	225
D.8	Data treatment for the calculation of reduction activation energy, E_r of VPOCr2.	226
D.9	Data treatment for the calculation of reduction activation energy, E_r of VPOZn2.	227
D.10	Data treatment for the calculation of reduction activation energy, E_r of VPDCo2.	228
D.11	Data treatment for the calculation of reduction activation energy, E_r of VPDCr2.	229
D.12	Data treatment for the calculation of reduction activation energy, E_r of VPDZn2.	230

LIST OF FIGURES

Figure		Page
1.1	Oxidation of <i>n</i> -butane to maleic anhydride via dehydrogenation and oxygenates insertion.	7
2.1	Idealised model of $(VO)_2P_2O_7$ at (100) plane showing only V and O.	21
2.2	Possible local structure modification of the $(VO)_2P_2O_7$ structure.	48
3.1	Physisorption isotherms and hysteresis loop types.	57
4.1	SEM micrographs for (a) VPO40, (b) VPO100 and (c) VPO132.	73
4.2	XRD diffractograms for VPOP in comparison with the standard.	75
4.3	XRD diffractograms VPO40, VPO100 and VPO132 in comparison with the standard.	76
4.4	Temperature-programmed desorption profile for VPO40, VPO100 and VPO132.	84
4.5	Temperature-programmed reduction profile for VPO40, VPO100 and VPO132.	88
5.1	SEM micrographs for (a) VPD75, (b) VPO75 and (c) VPA75.	97
5.2	XRD diffractograms for VPDP, VPOP and VPDP as a comparison to the standard.	99
5.3	XRD diffractograms for VPD75, VPO75 and VPA75 as a comparison to the standard.	101
5.4	Temperature-programmed desorption profile for VPD75, VPO75 and VPA75.	107
5.5	Temperature-programmed reduction profile for VPD75, VPO75 and VPA75.	111
6.1	SEM micrographs of (a) VPOCo2, (b) VPOCr2 and (c) VPOZn2.	122
6.2	SEM micrographs of (a) VPDCo2, (b) VPDCr2 and (c) VPDZn2.	124
6.3	XRD diffractograms for VPOCo2P, VPOCr2P and VPOZn2P as a comparison to the standard.	125
6.4	XRD diffractograms for VPDCo2P, VPDCr2P and VPDZn2P as a comparison to the standard.	127

6.5	XRD diffractograms for VPOCo ₂ , VPOCr ₂ and VPOZn ₂ as a comparison to the standard.	128
6.6	XRD diffractograms for VPDCo ₂ , VPDCr ₂ and VPDZn ₂ as a comparison to the standard.	131
6.7	Temperature-programmed desorption profile for VPOCo ₂ , VPOCr ₂ and VPOZn ₂ .	139
6.8	Temperature-programmed desorption profile for VPDCo ₂ , VPDCr ₂ and VPDZn ₂ .	142
6.9	Temperature-programmed reduction profile for VPOCo ₂ , VPOCr ₂ and VPOZn ₂ .	145
6.10	Temperature-programmed reduction profile for VPDCo ₂ , VPDCr ₂ and VPDZn ₂ .	148
6.11	Anaerobic temperature-programmed reaction profiles of <i>n</i> -butane/He over VPOCo ₂ .	151
6.12	Anaerobic temperature-programmed reaction profiles of <i>n</i> -butane/He over VPOCr ₂ .	152
6.13	Anaerobic temperature-programmed reaction profiles of <i>n</i> -butane/He over VPDCr ₂ .	153
B.1	Williamson-Hall plot for VPOP.	184
B.2	Williamson-Hall plot for VPO40.	185
B.3	Williamson-Hall plot for VPO100.	186
B.4	Williamson-Hall plot for VPO132.	187
B.5	Williamson-Hall plot for VPDP.	188
B.6	Williamson-Hall plot for VPOP.	189
B.7	Williamson-Hall plot for VPAP.	190
B.8	Williamson-Hall plot for VPD75.	191
B.9	Williamson-Hall plot for VPO75.	192
B.10	Williamson-Hall plot for VPA75.	193
B.11	Williamson-Hall plot for VPOCo ₂ P.	194
B.12	Williamson-Hall plot for VPOCr ₂ P.	195



B.13	Williamson-Hall plot for VPOZn2P.	196
B.14	Williamson-Hall plot for VPDCo2P.	197
B.15	Williamson-Hall plot for VPDCr2P.	198
B.16	Williamson-Hall plot for VPDZn2P.	199
B.17	Williamson-Hall plot for VPOCo2.	200
B.18	Williamson-Hall plot for VPOCr2.	201
B.19	Williamson-Hall plot for VPOZn2.	202
B.20	Williamson-Hall plot for VPDCo2.	203
B.21	Williamson-Hall plot for VPDCr2.	204
B.22	Williamson-Hall plot for VPDZn2.	205
C.1	Plot of $\ln(h/(\text{area})^2)$ versus $1/T$ for determination of desorption activation energy, E_d of VPO40.	206
C.2	Plot of $\ln(h/(\text{area})^2)$ versus $1/T$ for determination of desorption activation energy, E_d of VPO100.	207
C.3	Plot of $\ln(h/(\text{area})^2)$ versus $1/T$ for determination of desorption activation energy, E_d of VPO132.	208
C.4	Plot of $\ln(h/(\text{area})^2)$ versus $1/T$ for the determination of desorption activation energy, E_d of VPD75.	209
C.5	Plot of $\ln(h/(\text{area})^2)$ versus $1/T$ for the determination of desorption activation energy, E_d of VPO75.	210
C.6	Plot of $\ln(h/(\text{area})^2)$ versus $1/T$ for the determination of desorption activation energy, E_d of VPA75.	211
C.7	Plot of $\ln(h/(\text{area})^2)$ versus $1/T$ for the determination of desorption activation energy, E_d of VPOCo2.	212
C.8	Plot of $\ln(h/(\text{area})^2)$ versus $1/T$ for the determination of desorption activation energy, E_d of VPOCr2.	213
C.9	Plot of $\ln(h/(\text{area})^2)$ versus $1/T$ for the determination of desorption activation energy, E_d of VPOZn2.	214
C.10	Plot of $\ln(h/(\text{area})^2)$ versus $1/T$ for the determination of desorption activation energy, E_d of VPDCo2.	215



C.11	Plot of $\ln (h/(\text{area})^2)$ versus $1/T$ for the determination of desorption activation energy, E_d of VPDCr2.	216
C.12	Plot of $\ln (h/(\text{area})^2)$ versus $1/T$ for the determination of desorption activation energy, E_d of VPDZn2.	217
D.1	Plot of $\ln (h/(\text{area})^2)$ versus $1/T$ for determination of reduction activation energy, E_r of VPO40.	218
D.2	Plot of $\ln (h/(\text{area})^2)$ versus $1/T$ for determination of reduction activation energy, E_r of VPO100.	219
D.3	Plot of $\ln (h/(\text{area})^2)$ versus $1/T$ for determination of reduction activation energy, E_r of VPO132.	220
D.4	Plot of $\ln (h/(\text{area})^2)$ versus $1/T$ for determination of reduction activation energy, E_r of VPD75.	221
D.5	Plot of $\ln (h/(\text{area})^2)$ versus $1/T$ for determination of reduction activation energy, E_r of VPO75.	222
D.6	Plot of $\ln (h/(\text{area})^2)$ versus $1/T$ for determination of reduction activation energy, E_r of VPA75.	223
D.7	Plot of $\ln h$ versus $1/T$ for the determination of reduction activation energy, E_r , of VPOCo2.	224
D.8	Plot of $\ln h$ versus $1/T$ for the determination of reduction activation energy, E_r , of VPOCr2.	225
D.9	Plot of $\ln h$ versus $1/T$ for the determination of reduction activation energy, E_r , of VPOZn2.	226
D.10	Plot of $\ln h$ versus $1/T$ for the determination of reduction activation energy, E_r , of VPDCo2.	227
D.11	Plot of $\ln h$ versus $1/T$ for the determination of reduction activation energy, E_r , of VPDCr2.	228
D.12	Plot of $\ln h$ versus $1/T$ for the determination of reduction activation energy, E_r , of VPDZn2.	229
E.1	Adsorption-desorption isotherms of nitrogen at 77 K for (a) VPO40, (b) VPO100 and (c) VPO132.	230
E.2	BET plots for (a) VPO40, (b) VPO100 and (c) VPO132.	231
E.3	Adsorption-desorption isotherms of nitrogen at 77 K for (a) VPD75, (b) VPO75 and (c) VPA75 catalysts.	232

